

# Energy Expenditure Forecasting at Path Generation of Spherical Robots within Multi-Agent System

E. G. Borisov\*, R. U. Dobretsov and S. I. Matrosov

The Bonch-Bruевич Saint Petersburg State University of Telecommunications, Saint Petersburg, Russia;  
begspb1967@mail.ru

## Abstract

**Background:** The present research is relevant due to gathering the experience associated with a practical use of a spherical robot as a chassis for placing the local environmental monitoring equipment and due to the revealed need to use such robots within groups. Therefore, the article is aimed at showing the connections between the parameters of the external environment and kinematic, power and energy characteristics of the spherical robot chassis. **Method:** The main approaches to the research of the present problem are the methods of the transportation vehicle motion theory which in their turn are based on theoretical mechanics and theoretical physics laws, etc. The methodologies enable to significantly simplify a non-holonomic task associated with a sphere motion and to reach kinetic, power and energy characteristics appropriate for a practical use. **Findings:** The authors have studied the questions related to the estimation of energy expenditure for the spherical robot motion in an arbitrary path, have offered the concept of energy expenditure chart and shown the principles of using such chart for generation of a path of a spherical robot which operates within a multi-agent system. The approach regarding the generation of energy expenditure chart based on the preliminary area survey using a spherical robot has also been studied in the present article. **Improvements:** The materials of this article are of a practical value when working on the development of the ground component of multi-component multi-agent systems regardless of the type of the agent chassis.

**Keywords:** Controllability, Interaction of a Running Mover with Soil, Local Environmental Monitoring, Mobility, Multi-Agent System, Spherical Robot, Stability, Transport Task, Transportation Vehicle

## 1. Introduction

Spherical robot is of interest as a platform for placing the equipment of a local environmental monitoring, mainly when using it in the organized environment (industrial buildings and constructions, warehouses, rooms for the facilities of power-generating sector, airport territories and sites for the equipment storage, tunnel communications, etc)<sup>1</sup>. In this case it is possible to use positive aspects of a spherical robot, primarily omni-mobility, economic efficiency, compact size, ability to move afloat, high level of onboard equipment protection from the environment and relatively low cost.

Additionally to the environmental monitoring, the robots are capable of carrying out a patrol, reconnaissance and mapping or of monitoring the objects selected.

Much attention across the globe is paid to the question associated with using the spherical robots and with studying a smart use of different technical solutions when designing these robots<sup>2-18</sup>.

The article<sup>2</sup> presented an analytical summary of motion systems (drive system) of the spherical coordinate robots. The operational peculiarities of gyroscope and pendulum drive as well the advanced systems with an active shell, etc. was studied. Pendulum drive attracts the most practical interest in the context of our research. The methods of both the qualitative and quantitative comparison of the constructional solutions used at working on the spherical robots were offered in<sup>19</sup>.

This research work<sup>4</sup> dealt with the description of the constructions and the peculiarities of the implementation of motion systems with pendulum drive.

\* Author for correspondence

The sources<sup>5-11</sup> illustrated the solutions used by different development engineers and presented a vivid idea of the state-of-the-art constructions of the spherical robots.

The review of the publications over the last few years shows that researchers for the purpose of a quantitative analysis of kinematic, power and energy parameters of the spherical robot chassis, mainly use the traditional approaches of the theoretical mechanics in which rather sophisticated mathematical tools are used (refer to the articles<sup>12-18</sup>). But these approaches work well mainly when studying the motion along a rigid base. However, for solving the practical problems it is important to offer the methods which combine a relative simplicity of the calculations, sufficient accuracy and possibility to consider different types of motion surface.

The problem of a relatively low load capacity of a spherical robot can be solved by creating a heterogeneous group<sup>20</sup> of the spherical robots, which in its turn is an integral part of a single or multi-component multi-agent system<sup>20</sup>. The robots, making a group, support various sets of sensors and other equipment as well as the communication systems being different in power (even in physical principles) etc. i.e. an evident differentiation of the agents takes place. However, chassis are unified in terms of the technical features and capabilities of onboard control system. Additionally to a significant expanding of the operational capabilities, the use of a group increases a probability of task fulfillment due to a possibility to use the robots with the same functional capabilities in a group depending on a current number of agents and on the pattern of a current task.

The most effective approach turns out to be the implementation of a complex (combined) strategy which uses or the principles of centralized hierarchical control or the principles of decentralized group control<sup>20</sup>.

Standard procedures of the deployment of a minimal group of agents are shown in Figure 1.

The distance between the agents  $L$  is determined by a range of wireless communication. There has been implemented a bidirectional data communication between all the agents, which enables to use the strategy of decentralized group control. The experimental models of the robots are equipped with remote control, which enables to operate at a distance up to 50 m. After a while this distance will be increased.

The case of using all the agents of a multi-agent system

for studying the object of interest is shown in Figure 1a. This method of system deployment is preferable. The machine, the most closely located to the control station, is selected as a master-robot.

As the object of interest moves away, a group has to sacrifice the monitoring efficiency and use one or two agents as repeaters (Figure 1b, c). Since any robot of the group is capable of performing the functions of a master-robot, the robustness of a group increases. The failure of a master robot of the group in case of an impact of the object of interest does not result in group failure. The robustness of a group enhances with the increase of the agent numbers. In case of loss of radio signal with control station, the scenario of an autonomous operation mode of a group with a consequent return of the machine to a base station is foreseen.

The method of two-component system deployment is shown in Figure 1: Communication between a group and control station is maintained by using a drone.

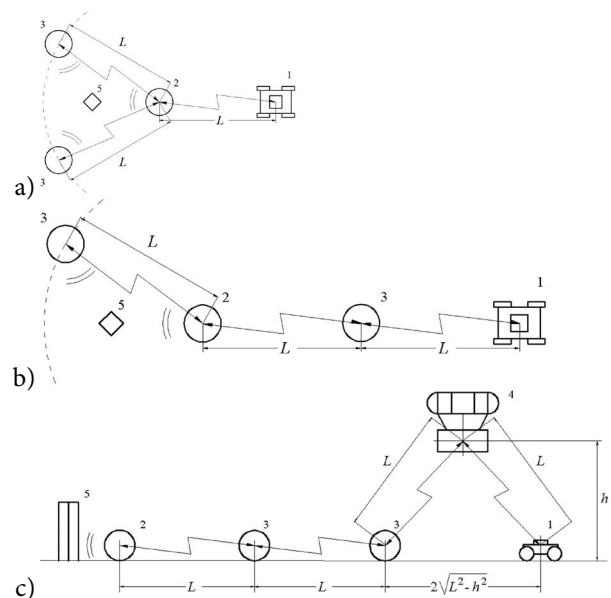


**Figure 1.** Basic methods of system deployment: a. Object investigation; b. Remote object investigation; c. Operation at minimum distance; 1. Mobile control station (point); 2. Master-robot; 3. Slave-robot; 4. Additional repeater; 5. Object of interest;  $L$ . Maximum permissible distance between agents;  $h$ . Repeater lift height.

Transport platform with a monospherical running gear (Figure 2)<sup>1,19,20</sup> which implements a motion principle being close to a motion principle of a monowheel, is used as a chassis of the agents.

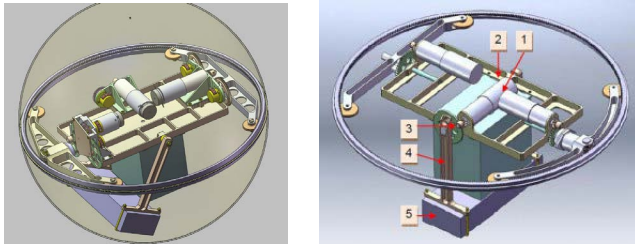


**Figure 2.** The principle of control of the spherical robot motion by means of pendulum deviation (on the left) and elements of the pendulum drive arrangement (on the right): 1. Drive; 2. Frame; 3. Additional fixed axle transmission; 4. Pendulum lever; 5. Accumulator storage battery (pendulum weight).

The control is performed by the deviation of pendulum drive. Pendulum position is controlled by electric motors in three independent planes. Power is supplied from two accumulator storage batteries which perform the function of the pendulum weight. The shell is made of optically transparent impact resistant plastic which enables to install a video camera on the platform.

There was made a group consisting of three spherical robots with the following characteristics: Weight is up to 4 kg, shell outside diameter is 0.4 m, speed on a horizontal surface is up to 2 m/sec, height of the obstacles avoided by the robots is more than 10 mm, calculated lift angle is not less than  $5^\circ$ , operational duration in autonomous mode is up to 10 hours.

## 2. Concept Headings

One of the main tasks which directly provide the efficiency of the group operation is the automated generation of the agent paths. In the optimal control theory the problem is known as a “transport task”. For the automated generation of the machine path there was tested Lee algorithm. The other related methods can also be used for this purpose<sup>13</sup>.

At the evaluation of the control system operation associated with the task of path generation, normally the time spent on search of a solution and the time for performing the maneuver in the field is taken into consideration. However, an important parameter for monitoring system is the duration of the operation in autonomous mode; therefore the energy expenditure question should also be taken into consideration at performing the current task. In some cases, it is expedient to perform the path optimization not based on minimum

time for the task performance but based on minimum energy expenditure for this.

Consequently, the purpose of this article is to offer the method of the estimation of energy expenditure for the spherical coordinate robot chassis at motion along the arbitrary path considering the necessity to provide the operation in the group.

## 3. Results

In order to perform the automated generation of chassis path using Lee algorithm or relative to it, the ground map is divided into cells with dimensions determined by the typical geometrical dimensions of the transportation vehicle (for example, overall dimensions) and as a result, so called digital work field is obtained<sup>21</sup>. In case with a spherical robot, the cells of the field have a square shape and the length of a side is equal to the outside diameter of a sphere. The cells are divided into groups of cells forbidden for motion and cells permitted for motion. The cells of the first group are considered to be impassable for chassis and the path should be generated with avoiding such cells. If the value “1” is associated with the numbers of these cells, then the value “0” is associated with the numbers of the cells of the second group. As a result of the execution of path generation algorithm in case when the task has a solution, it is possible to obtain one or several paths. Traditionally, the shortest path is selected. The path presents a broken line consisting of the straight legs the length of which, in the simplest case, is equal to the outside diameter of a sphere. Specificity of the set of agents is taken into consideration by means of the dynamic update of the maps, at which the other robots involved in the group operation are marked on the map as impassable obstacles.

Thus, for each path option it is possible, by calculation, to estimate energy expenditure for chassis motion, knowing the supporting surface characteristics (in a broader sense – knowing the motion conditions). For this purpose in general case, a non-holonomic task of the theoretical mechanics about the rolling motion of a sphere will be substituted with a holonomic one and slippage effect on kinematic, power and energy system parameters will be taken into consideration, when required, using the trial coefficients of rolling resistance and frictional sliding. In the theory of transportation vehicle motion such approach enables to discretely evaluate the

parameters of chassis motion with a reasonable accuracy. Correspondently, there has been gained a methodological experience of prediction of the motion parameters of the wheeled and tracked vehicles and a spherical robot can be considered as a mono-wheeled platform.

The input parameters of the mathematical model will be the motion conditions (rolling resistance coefficient, friction coefficient, supporting surface slope angle, velocity of the air stream blowing off the machine) and main weight-and dimensional chassis characteristics.

Chassis power balance is as follows:<sup>22</sup>

$$P_k = P_\psi + P_w + P_j,$$

where  $P_k$  – tractive power ;  $P_\psi$  – road resistance;  $P_w$  – air resistance;  $P_j$  – inertia force of motion resistance.

Integral parts of the power balance are determined according to the following dependencies.

Tractive power is determined based on the following expression  $P_k = M_k/R = a mg \sin \gamma/R$ , where  $M_k$  – torque moment,  $R$  – sphere radius,  $m$  and  $a$  – pendulum weight and radius,  $\gamma$  – pendulum deviation angle,  $g = 9.81 \text{ m/sec}^2$  – gravitational acceleration.

Frictional sliding coefficient is determined according to the empirical dependence:

$$\sigma = -(0,03...0,05) \frac{P_k}{\phi R_z} \ln \left( 1 - \frac{P_k}{\phi R_z} \right)$$

Here  $\phi$  – friction coefficient known for this surface and for the normal reaction the following equation holds true:  $R_z = G$  ( $G$  – chassis weight).

Consequently, considering the frictional sliding:

$$P_k^* = P_k / (1 - \sigma).$$

Rolling resistance  $P_\psi = G(f \cos \alpha \pm \sin \alpha) = G\psi$ . Here  $f$  – rolling resistance coefficient (at which in general case, soil distortion, rutting formation losses, etc. are taken into consideration),  $\alpha$  – lift or slope angle passed by the robots,  $\psi$  – motion resistance coefficient.

At motion on the distorted soil the rolling resistance increases. An important feature of the spherical robot running mover is a significant dependency of the contact area with supporting base on the characteristic of the supporting base itself. Though on the whole, the spherical robot constructions made are characterized by a very low soil pressure which excludes causing the damage to the major cohesive soils, the pattern of the normal load

transmission is different from the cases with wheeled and tracked running gears. The closest analogue turns out to be a cylinder-conic wheel used in the construction of the planetary rover<sup>23</sup> and offered as a part of a running gear of the reconnaissance wheeled walking machine.

Design model used at simulation of robot sinking into the deformed soil is shown in Figure 3. We will select the contact area load distribution law. As the experience of simulation of the normal reactions under the roller of the tracked machine<sup>24</sup> using the distribution diagrams shows, studying the “flat” case gives good results with the distributed load representation in the form of a parabola with maximum in the geometrical center of the contact area (refer to Figure 3).

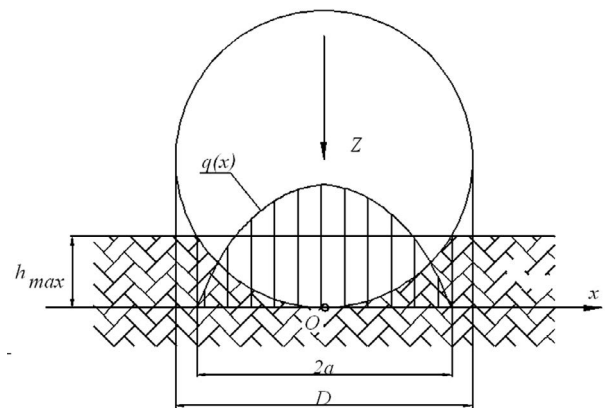


Figure 3. Parabolic approximation of a distributed load.

Thus, a parabolic law of the load distribution along the contact spot gives the following dependency:  $q(x) = k \cdot (a^2 - x^2)$ , where  $k = 0,75Z/a^3$  – a coefficient selected from the condition:

$$\int_{-a}^a q(x) dx = Z.$$

Here  $Z$  – a vertical load on a sphere (in the simplest case  $Z=G$ , where);  $a$  – radius of an imprint on the soil.

Average pressure on the soil can be determined as a correlation between a vertical load on a sphere and a square of a spherical segment sunk into the soil.

We will define as follows:  $h$  – segment height,  $r$  – segment base radius,  $h_{max}$  – sinking depth,  $D$  – sphere diameter.

Spherical segment square (properly cut off spherical surface):

$$S_{segm} = \pi(h^2 + r^2).$$

Thus, the square of the contact area (contact spot) in the definition used in Figure 1 for a sphere on the distorted soil and average pressure on the ground are as follows:

$$F_K = \pi(h^2 + 4a^2) \text{ and } q_{cp} = \frac{Z}{\pi(h_{max}^2 + 4a^2)}.$$

Based on the geometrical constructions it is possible to obtain the relation between imprint radius and the deepest sinking (Figure 3):

$$h_{max} = 0,5 \cdot (D - \sqrt{D^2 - 4a^2}). \tag{1}$$

The expression (1) enables to obtain and use the dependency at calculation of an average normal pressure:

$$a = \sqrt{(D - h_{max}) \cdot h_{max}}. \tag{2}$$

Using the understandings, accepted in the transport machinery of the relation between the load and distorted soil settlement we will write as follows:

$$q(x) = (k_c + bk_\phi) [z(x)]^n.$$

Here  $z(x)$  – soil distortion at applying a vertical load  $q(x)$ ;  $k_c, k_\phi, n$  – empirical coefficients the soil distortion settlement is characterized by at applying a vertical load on a stamp with width  $b$ .

In case with a sphere, a typical size of a stamp is a diameter, thus,  $b = 2a$ , consequently:

$$h_{max} = \sqrt[n]{\frac{q_{max}}{(k_c + bk_\phi)}}.$$

Maximum value of a vertical load is:  $q_{max} = 0,75Z/a$ .

We obtain as follows:

$$h_{max} = \sqrt[n]{\frac{0,75Z/a}{(k_c + bk_\phi)}}. \tag{3}$$

Simultaneous solution of the Equations (1) and (2) enables to determine (knowing the values of the parameters  $k_c, k_\phi, n$ ) the values  $a$  and  $h_{max}$ .

Parameters of sandy soil:<sup>25,26</sup>

$$k_c \approx 2,3 \text{ kg/cm}^{1+n}; k_\psi \approx 0,2 \text{ kg/cm}^{2+n}; n \approx 0,42. \tag{4}$$

Simultaneous solution (1) and (3) at substitution (4) was made numerically. At evaluation of the depth of sinking into sand of a spherical robot with weight of 4 kg and with sphere diameter of 0.4 m the following values were obtained  $a = 43 \text{ mm}$  and  $h_{max} = 5 \text{ mm}$ .

The results of the calculations of an average normal pressure for different values of sphere radius and machine weight are listed in Table 1.

**Table 1.** Dependencies  $q_{cp}(m, R)$  on sandy soil with parameters  $k_c \approx 2,3 \text{ kg/cm}^{1+n}$ ;  $k_\psi \approx 0,2 \text{ kg/cm}^{2+n}$ ;  $n \approx 0,42$ .

$q_{cp}(m, R)$ , kg/cm <sup>2</sup>		Chassis weight, kg			
		4	6	8	10
Sphere radius, m	0.2	0.17	0.22	0.26	0.31
	0.4	0.12	0.16	0.19	0.23
	0.6	0.10	0.13	0.16	0.18

Rolling resistance coefficient is as follows:

$$f_s = \frac{P_{\#}}{R_z} = \frac{b \int_0^{h_{max}} p_s dh}{R_z} = \frac{b \int_0^{h_{max}} \frac{P_z}{\pi(h^2 + 4a^2)} dh}{R_z} = \frac{bh_{max}}{\pi(h^2 + 4a^2)}.$$

For soil with characteristics considered, the value of motion resistance coefficient will make 0.22.

Aerodynamic resistance in general case is determined as follows:  $P_w = cpFV^n$ , where  $c = 0.25$  – a non-dimensional coefficient of the sphere aerodynamic resistance;  $\rho = 1.25 \text{ kg/m}^3$  – air density;  $F = \pi R^2$  – midsection of the robot body;  $V$  – center-of mass velocity (or normal velocity component of the air stream blowing off a chassis). At low speed (up to 1 m/sec)  $n = 1$  is taken. At high speed  $n = 2$  is taken. Inertia force is determined as a difference  $P_j = P_k - (P_\psi + P_w)$  and in this case, it characterizes chassis acceleration capability. At steady motion this force tends to zero.

Graphical representation of power balance is shown in Figure 4.

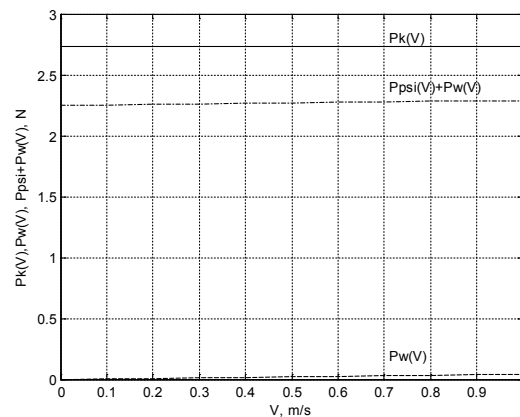


**Figure 4.** Power balance of a spherical robot at lifting motion of 3°.

Calculated dependencies were obtained by analogy with the dependencies traditional for the theory of the wheeled vehicle motion considering the peculiarities of the spherical robot construction.

Thus, energy expenditure for chassis motion based on the action of the external forces can be determined as follows:

$$\Delta E_{\psi} = \sum_{j=1}^l (P_{\psi_j}^* D) = D \sum_{j=1}^l P_{\psi_j}^* .$$

Here  $l$  – number of broken line legs with length  $D$  the considered path is composed of.

Passage of obstacles is also accompanied by energy losses. For obstacles with height of up to 10 mm we can restrict ourselves to the case of chassis potential energy change:

$$\Delta E_h = \sum_{j=1}^l (mgH_j) = mg \sum_{j=1}^l H_j .$$

Typification of obstacles (irregularities) is given in Table 2<sup>1</sup>.

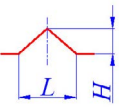
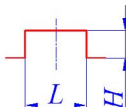
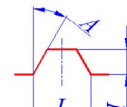
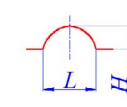
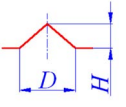
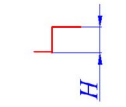
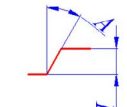
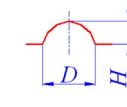
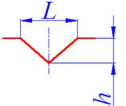
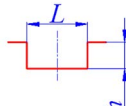
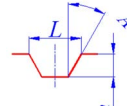
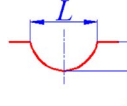
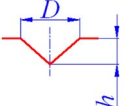
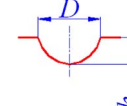
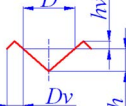
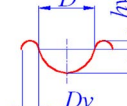
As one can see from Table 2, each obstacle can be represented in the form of a combination of the typical elements: combination of rifts, ravines (channels and moats) and sloping surfaces.

Thus, energy expenditure on the path selected can be determined as a sum of as follows:

$$\Delta E = \Delta E_{\psi} + \Delta E_h .$$

For automation of the estimation of energy expenditure on the path we offer to use energy expenditure chart generated based on the calculations or experimentally obtained. Energy expenditure chart as well as trafficability map is based on the discrete work filed with size  $(n+1) \times (m+1)$ , with square cells and side length equal to sphere diameter (Figure 5).

**Table 2.** Cross section of irregularities

Irregularities in land surface	Shape of irregularities			
	Triangular	Rectangular	Trapezoidal	Rounded
Stone, earth barrier				
Hill, step				
Ditch				
“Crater” without earth barrier		-	-	
“Crater” with earth barrier		-	-	

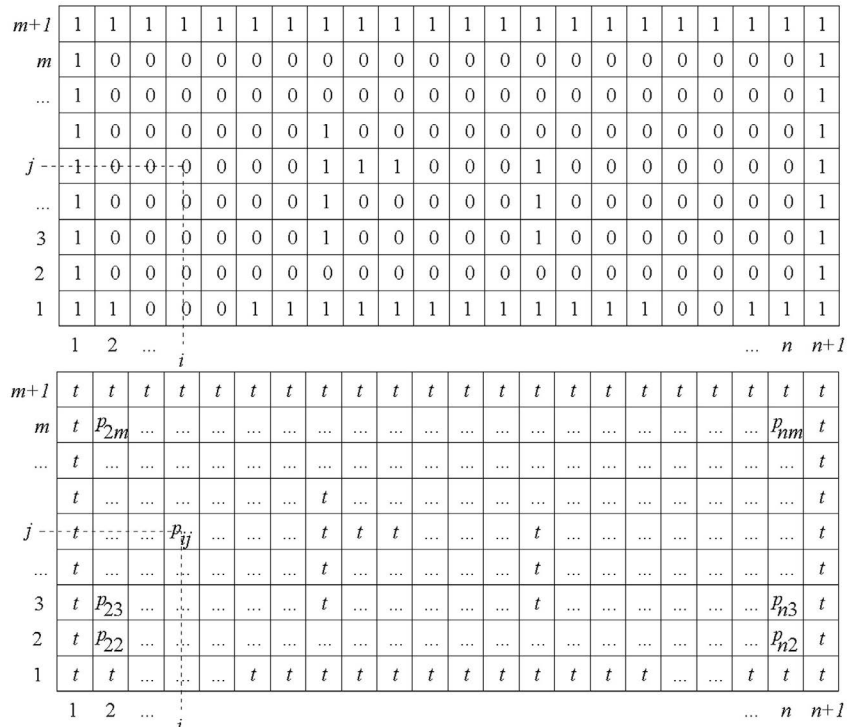


**Figure 5.** Geometrical interpretation of discrete work field in the form of a chart and map: above – trafficability map; below – energy expenditure chart.

Differently from the cells of trafficability map, each cell of energy expenditure chart is characterized by four parameters making vector  $p_j$ . Each of these parameters characterizes the relative energy expenditure at going through the cell in one of four directions (parallel to axis of coordinates). In the simplest case (at the absence of a significant aerodynamic resistance of the environment), it is a ratio of the coefficient of motion resistance  $\psi$  for this cell to the coefficient of rolling resistance  $f_0$  of a robot on a horizontal rigid surface. If the cell is impassable for a chassis a parameter takes some  $t$  value which exceeds energy capabilities of the machine (Figure 6).

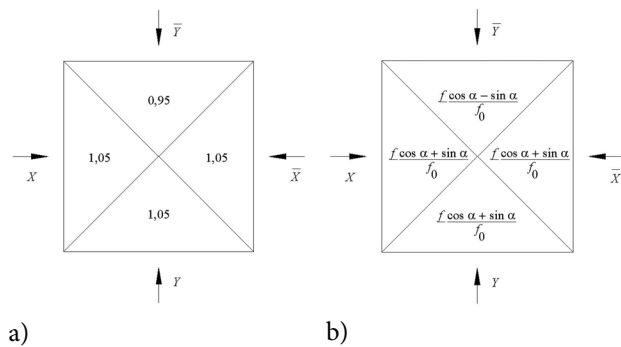


**Figure 6.** Graphical representation of the cell of energy expenditure chart: a. Concretely defined; b. With symbolic description.

Energy expenditure chart can be directly used as a basis for path generation using the same data processing algorithms which were used for trafficability map. Decrease of the number of calculation operations at estimation of energy expenditure for motion in a path is an advantage.

For the experimental generation of energy expenditure chart, each cell in the discrete work field should be passed by a chassis at least once in each of four directions. Energy expenditure can be determined using the opportunity when the torque moment developed by the electric motor is directly proportional to the current strength. Knowing the motion speed  $v$ , it is possible (for a uniform motion) to write as follows:

$$(\Delta E_\psi)_{ij} = UID / (v\eta_{mech}).$$

Here  $U$  and  $I$  – onboard voltage and current strength in the circuit of the tractive drive motor  $\eta_{mech}$  – efficiency coefficient of the drive gear system (constant value). At constant speed and constant power supply voltage, relative expenditure will be equal to current ratio at the consumption of current by the tractive drive motor at going through this cell and at motion on a rigid surface.

Total energy expenditure (knowing the relevant values of the mechanical efficiency coefficient of gear

parts of the robot drive) can be determined by addition of energy expenditure for three drives used in the motion system. However, it should be noted that the main energy consumer will not be the system of the robot motion but onboard equipment.

## 4. Discussion

As opposed to the known approaches to the robot motion simulation, in the present article we offer to use the methods developed based on the theory of the wheeled vehicle motion. This enables to significantly simplify the calculations.

Energy expenditure chart embodies the development of the principle associated with using the feature charts (used for decreasing the calculation volumes in the systems of the electronic control of different equipment including a motor, car gear box) and trafficability maps (developed for automation of the machine path generation). The use of energy expenditure chart enables to simplify the generation of a path on which the least energy consumption is expected and also enables to maintain a possibility to generate as short paths as possible.

The principle of the experimental generation of energy expenditure charts enables to simplify and automate this procedure.

## 5. Conclusion

- The estimation of energy expenditure can be used at selecting the method of path generation of the transportation vehicle operating as in an autonomous mode as well as within homogeneous and non-homogeneous groups.
- The use of energy expenditure charts offered in the present article enables to simplify the calculations and generate a path in an automation mode. Both assignment and solution of a task, associated with transportation vehicle path generation, become possible under the principle of cost-effectiveness which is relevant at conducting the monitoring.
- Energy expenditure charts can be generated as based on the calculations as well as experimentally. In the latter case, the charts are generated for example, based on data on the current strength of electric drives of a spherical robot which, according to some algorithm,

goes through all the work field cells available for motion.

Generation of energy expenditure chart is possible using the machines developed for solution of the main group task (conducting the local environmental monitoring) and does not require significant computational capabilities. The use of the charts implies the possibility of working with time-tested algorithms of path generation. Thus, a practical implementation of the offer hereinbefore expressed seems to be possible.

## 6. Acknowledgement

The present research work has been carried out with financial support from the Ministry of Education and Science of the Russian Federation in the frames of the federal targeted program “Research and Development in the Priority Areas for the Development of Science and Technology Sector of the Russian Federation for 2014-2020” pursuant to the project: “Development of the Adaptive Control Methods and Algorithms of Multi-Agent Spherical Robot Motion with Increased Maneuvering Capability under Uncertainty and Significant External Disturbances” (Unique Project Identifier RFMEFI61315X0047).

## 7. References

1. Dobretsov RU, Borisov EG, Kucherenko VI, Bogachev AN, Matrosov SI. Spherical robot as a platform for ecological monitoring. *Transport. Transport Infrastructure and Facilities. Ecology.* 2015; 3:35–50.
2. Chase R, Pandya A. A review of active mechanical driving principles of spherical robots. *Robotics.* 2012; 1:3–23. DOI: 10.3390/robotics1010003.
3. Sheng Z, Xiang F, Shouqiang Z, Kai D. Kinetic model for a spherical rolling robot with soft shell in a beeline motion. *Journal of Multimedia.* 2014 Feb; 9(2):223–9. DOI: 10.4304/jmm.9.2.223-229.
4. Ch Y, Guo S, Shi L. Hydrodynamic analysis of the spherical underwater robot SUR-II. *International Journal of Advanced Robotic Systems.* 2013; 10(247):1–12. DOI: 10.5772/56524.
5. ROSPHERE spherical robot. 2013. 2016. Available from: [http://www.prorobot.ru/09/ROSPHERE\\_shar.php](http://www.prorobot.ru/09/ROSPHERE_shar.php)
6. Hernandez JD, Barrientos J, del Cerro J, Barrientos A, Sanz D. Moisture measurement in crops using spherical robots. *Industrial Robot: An International Journal.* 2013; 40:59–66. DOI: 10.1108/01439911311294255.
7. Ground Bot. 2016. Available from: <http://www.rotundus.se/>

8. 2016. Available from: [http://www.unusuallocomotion.com/medias/images/thisthe-sphere-robot-1993.jpg?fx=r\\_900\\_900](http://www.unusuallocomotion.com/medias/images/thisthe-sphere-robot-1993.jpg?fx=r_900_900)
9. Gigantic Robotic Ball. 2016. Available from: <https://www.flickr.com/photos/daikiki/3596965040/>
10. Hopping Robots (RATS). 2016. Available from: <http://www.nrec.ri.cmu.edu/projects/rats/>
11. Morp Hex MK-II in Action! 2014. 2016. Available from: <http://blog.trossenrobotics.com/2014/03/19/morphex-mk-ii-in-action/>
12. Ocampo-Jimenez J, Munoz-Melendez A, Rodriguez-Gomez G. Extending a spherical robot for dealing with irregular surfaces: A sea urchin-like robot. *Advanced Robotics*. 2014; 28(22):1475–85. DOI: 10.1080/01691864.2014.968615.
13. Fujioka J, Nakamura S, Seki H. Development and control of all direction jumping and rolling spherical robot. *Transactions of the JSME (in Japanese). Dynamics and Control, Robotics and Mechatronics*. 2016; 82(833):1–15. DOI: 10.1299/transjsme.15-00146.
14. Gajbhiye S, Banavar RN. Geometric modeling and local controllability of a spherical mobile robot actuated by an internal pendulum. *International Journal of Robust and Nonlinear Control*. 2016; 26(11):2436–54. DOI: 10.1002/rnc.3457.
15. Li T, Wang Z, Ji Z. Dynamic modeling and simulation of the internal- and external-driven spherical robot. *Journal of Aerospace Engineering*. 2012; 25(4):636–40. DOI: 10.1061/(ASCE)AS.1943-5525.0000158.
16. Hogan F, Forbes J, Barfoot T. Rolling stability of a power-generating tumbleweed rover. *Journal of Spacecraft and Rockets*. 2014; 51(6):1895–906. DOI: 10.2514/1.A32883.
17. Karavaev YL, Kilin AA. The dynamics and control of a spherical robot with an internal omniwheel platform. *Regular and Chaotic Dynamics*. 2015 Mar; 20(2):134–52. DOI: 10.1134/S1560354715020033.
18. Chen WH, Chen ChP, Yu WSh, Lin ChH, Lin PCh. Design and implementation of an omnidirectional spherical robot omnicon. *Mechanism and Machine Theory*. 2013 Oct; 68:35–48. DOI: 10.1016/j.mechmachtheory.2013.04.012.
19. Dobretsov RU, Borisov EG, Matrosov SI. About selection of the drive type for a spherical robot. *Transport Infrastructure and Facilities. Ecology*. 2016; 2:17–29.
20. Borisov EG, Dobretsov RU, Matrosov SI. About the ground multi-agent system based on the group of spherical robots. *Proceedings of the International Science and Technology Conference Transport and Transport-Technological Systems*; Tyumen: Tyum GNGU. 2016. p. 32–7.
21. Avotin EV, Dobretsov RU. Automation control of transportation vehicles: Study guides for universities and colleges majoring in “Automotive and Tractor Industry”. Saint Petersburg: State Polytechnical University Press; 2013.
22. Dobretsov RU, Vasilyev IV. Force and power balance of a spherical running gear. *Proceedings of the International Forum Science Week, Saint Petersburg State Polytechnical University. The Institute of Energy and Transport Systems. Part I*. Saint Petersburg: State Polytechnical University Press; 2015. p. 30–3.
23. Avotin EV, Dobretsov RU, Matrosov SI. Adaptive chassis of spherical robots. *Scientific and Technical Reports. Saint Petersburg State Polytechnical University. Ser: Science and Education*. 2013; 3(178):230–7.
24. Dobretsov RU. Regarding the question of a theoretical evaluation of performance characteristics of the track-type vehicle chassis. *Scientific and Technical Reports. Saint Petersburg State Polytechnical University, Ser: Science and Education*. 2011; 3:98–103.
25. Avotin EV, Dobretsov RU. Methods of calculation of energy expenditure for the wheeled vehicles. *Scientific and Technical Reports. Saint Petersburg State Polytechnical University. Ser.: Science and Education*. 2012; 4(159):168–72.
26. Avotin EV, Dobretsov RU. Calculation methods of normal pressure on the ground contacting area of track of the transportation vehicle. *Scientific and Technical Reports. Saint Petersburg State Polytechnical University. Ser: Science and Education*. 2011; 3:103–8.